AMERICAN SOCIETY FOR MICROBIOLOGY | mBio®

RESEARCH ARTICLE

# Calcium-Responsive Diguanylate Cyclase CasA Drives Cellulose-Dependent Biofilm Formation and Inhibits Motility in *Vibrio fischeri*

**Alice H. Tischler,[a]* Michael E. Vanek,[a] Natasha Peterson,[a] Karen L. Visick[a]**

[a]Department of Microbiology and Immunology, Loyola University Chicago, Maywood, Illinois, USA

**ABSTRACT** The marine bacterium *Vibrio fischeri* colonizes its host, the Hawaiian bobtail squid, in a manner requiring both bacterial biofilm formation and motility. The decision to switch between sessile and motile states is often triggered by environmental signals and regulated by the widespread signaling molecule c-di-GMP. Calcium is an environmental signal previously shown to affect both biofilm formation and motility by *V. fischeri*. In this study, we investigated the link between calcium and c-di-GMP, determining that calcium increases intracellular c-di-GMP dependent on a specific diguanylate cyclase, calcium-sensing protein A (CasA). CasA is activated by calcium, dependent on residues in an N-terminal sensory domain, and synthesizes c-di-GMP through an enzymatic C-terminal domain. CasA is responsible for calcium-dependent inhibition of motility and activation of cellulose-dependent biofilm formation. Calcium regulates cellulose biofilms at the level of transcription, which also requires the transcription factor VpsR. Finally, the *Vibrio cholerae* CasA homolog, CdgK, is unable to complement CasA and may be inhibited by calcium. Collectively, these results identify CasA as a calcium-responsive regulator, linking an external signal to internal decisions governing behavior, and shed light on divergence between *Vibrio* spp.

**IMPORTANCE** Biofilm formation and motility are often critical behaviors for bacteria to colonize a host organism. *Vibrio fischeri* is the exclusive colonizer of its host's symbiotic organ and requires both biofilm formation and motility to initiate successful colonization, providing a relatively simple model to explore complex behaviors. In this study, we determined how the environmental signal calcium alters bacterial behavior through production of the signaling molecule c-di-GMP. Calcium activates the diguanylate cyclase CasA to synthesize c-di-GMP, resulting in inhibition of motility and activation of cellulose production. These activities depend on residues in CasA's N-terminal sensory domain and C-terminal enzymatic domain. These findings thus identify calcium as a signal recognized by a specific diguanylate cyclase to control key bacterial phenotypes. Of note, CasA activity is seemingly inverse to that of the homologous *V. cholerae* protein, CdgK, providing insight into evolutionary divergence between closely related species.

**KEYWORDS** diguanylate cyclase, *Vibrio cholerae*, *Vibrio fischeri*, biofilms, calcium sensors, calcium signaling, cellulose, cyclic nucleotides

Bacteria adapt to their surroundings by recognizing environmental signals, resulting in changes in gene expression, protein production and/or activity, and other processes that permit them to survive and/or thrive accordingly. In some cases, adaptation promotes development of biofilms, sessile communities encased within a protective extracellular matrix. Biofilms provide fitness advantages based on social cooperation, resource sharing, and protection from environmental stressors, such as antibiotics (1, 2). Planktonic cells sense and respond to signals by first adhering to surfaces, typically via flagella or other surface structures. Attached cells then produce and secrete the

**Citation** Tischler AH, Vanek ME, Peterson N, Visick KL. 2021. Calcium-responsive diguanylate cyclase CasA drives cellulose-dependent biofilm formation and inhibits motility in *Vibrio fischeri*. mBio 12:e02573-21. https://doi.org/10.1128/mBio.02573-21.

**Editor** Joerg Graf, University of Connecticut



Address correspondence to Karen L. Visick, kvisick@luc.edu.

*Present address: Alice H. Tischler, Department of Molecular Biology and Microbiology, Tufts University Medical Center, Boston, Massachusetts, USA.

**Received** 30 August 2021
**Accepted** 28 September 2021
**Published** 9 November 2021

protective matrix, leading to additional advantageous changes in cellular physiology. These stages of biofilm development are regulated by both environmental and internal signals, with multiple inputs allowing for fine-tuned control (1).

In many bacteria, internal signaling relies on cyclic dinucleotides, such as bis(3′-5′)-cyclic dimeric GMP (c-di-GMP), a small widespread second messenger that regulates numerous bacterial behaviors, including biofilm formation, motility, and virulence (3, 4). c-di-GMP is synthesized by diguanylate cyclases (DGCs), which contain a GGDEF domain, and is degraded by phosphodiesterases (PDEs), containing either EAL or HD-GYP domains (5–7). Although the number of DGCs and PDEs encoded within bacterial genomes can differ greatly, many organisms contain dozens of such genes, highlighting the importance of c-di-GMP as an intracellular signal (3).

c-di-GMP was first discovered as an activator of bacterial cellulose synthase (8). Since then, c-di-GMP has been implicated in activation of numerous polysaccharides in a variety of species at multiple levels of control. For example, in *Vibrio cholerae*, c-di-GMP activates the *Vibrio* polysaccharide (*vps*) locus through binding and increasing activity of transcriptional regulators VpsR and VpsT (9–12). Activation of polysaccharide production by c-di-GMP is often linked to environmental signals and signal transduction, and sensory domains are commonly associated with DGCs and PDEs (3). This variety of sensory domains is matched by the diversity of known signals that impact c-di-GMP. For example, in *V. cholerae* alone, known signals include temperature, bile acids, polyamines, and ferrous iron (9, 13–16).

Calcium is one environmental signal linked to c-di-GMP and known to impact bacterial biofilm formation. In marine *Vibrio* spp., the level of calcium present in seawater (10 mM [17]) exerts both negative (*V. cholerae* [18]) and positive (*V. vulnificus* [19] and *V. fischeri* [20]) effects on biofilm formation, all through different mechanisms. In *V. cholerae*, the calcium-sensing two-component system CarRS decreases transcription of *vpsR*, resulting in decreased *vps* transcription and biofilm formation (18). In *V. vulnificus*, calcium increases c-di-GMP, increasing transcription of the biofilm and rugose polysaccharide (*brp*) locus, dependent on both the IamA pilin and VpsR homolog, BrpR (19, 21, 22). The calcium-binding matrix protein CabA, which is also induced by calcium, contributes to rugosity and matrix structure (23, 24). In *V. fischeri*, calcium coordinately induces transcription of genes for the synthesis of two polysaccharides known to contribute to biofilm formation, *bcs* (cellulose) and *syp* (symbiosis polysaccharide [SYP]) (20). The mechanism by which calcium increases transcription of polysaccharide loci and induces biofilm in *V. fischeri* is as yet unknown; the *V. fischeri* genome lacks homologs of known calcium-sensing systems present in the other *Vibrio* spp. Calcium also inhibits *V. fischeri* motility, a behavior considered to be the opposite of sessile biofilm formation (25). While motility control has been associated with changes in c-di-GMP levels, the mechanism by which calcium inhibits motility also is unknown (25, 26). Understanding how *V. fischeri* biofilm formation and motility are controlled in response to environmental signals, specifically calcium, is important, as both phenotypes represent key behaviors that are required for symbiotic colonization by *V. fischeri* of its host organism, the Hawaiian bobtail squid, *Euprymna scolopes* (27–29).

In this study, we investigated the link between calcium and c-di-GMP in *V. fischeri*, determining that calcium increases c-di-GMP through the activation of DGC CasA. Activated CasA, in turn, inhibits motility and drives cellulose-dependent biofilm formation. Additionally, investigation of the *V. cholerae* homolog CdgK suggested that CdgK may be inhibited by calcium. Collectively, these results identify CasA as an important regulator and illustrate how integration of calcium and c-di-GMP signals affect bacterial behaviors.

## RESULTS

**Calcium increases c-di-GMP in *V. fischeri*.** In *V. vulnificus*, calcium induces biofilm formation through an increase in c-di-GMP (19). Because calcium also induces biofilm formation by *V. fischeri* (20), we hypothesized that calcium could cause an increase in c-di-GMP. To investigate this possibility, we utilized an intracellular c-di-GMP biosensor

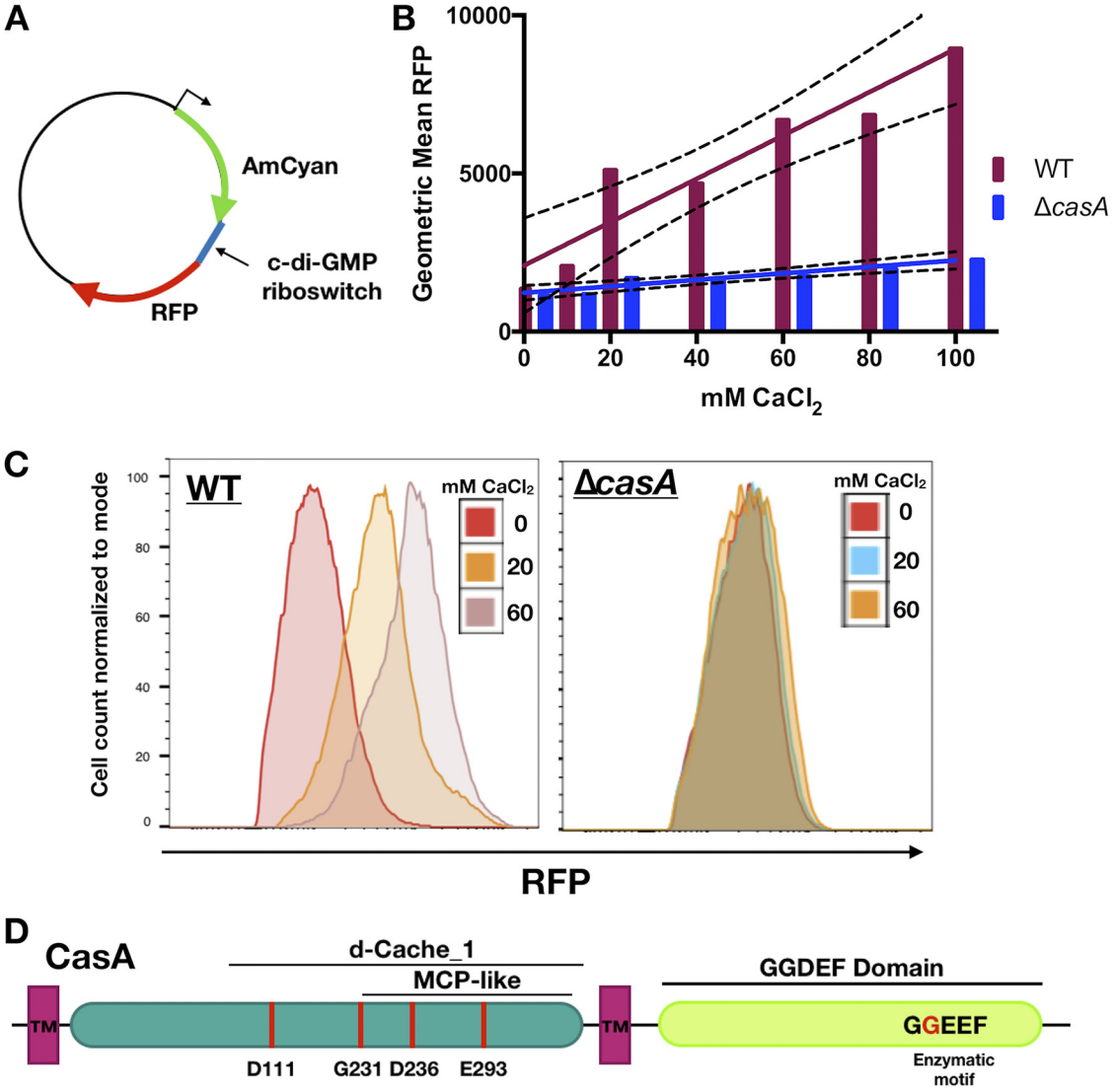


**FIG 1** CasA increases intracellular c-di-GMP in response to calcium. (A) Schematic of pFY4535 c-di-GMP biosensor plasmid, which contains a constitutive AmCyan cassette and a c-di-GMP binding riboswitch that controls Turbo-RFP expression. (B) Geometric mean of RFP, the area under the curve as determined via flow cytometry for ES114 (WT) and Δ*casA* (KV9179) containing the pFY4535 biosensor plasmid. Data points represent three biological replicates at increasing concentrations of $CaCl_2$ as indicated. Solid lines indicate linear regression fitted slope lines, and dashed lines indicated the confidence interval. Linear regression analysis determined the slopes are significantly different from each other ($P = 0.0001$). (C) Representative histograms showing $AmCyan^+$ $RFP^+$ live cells, with cell count normalized to mode. The *x* axis shows increasing RFP. The left histogram represents ES114 (WT), and the right represents the Δ*casA* mutant (KV9179), both strains containing plasmid pFY4535. (D) Schematic of general CasA protein structure. Two transmembrane regions flank an N-terminal sensory domain (teal) with predicted dCache-1 and MCP-like domains. The C-terminal domain consists of a GGDEF DGC domain containing an enzymatic GGEEF motif. Red lines and letters indicate substituted residues. All locations are approximate and not to scale.

in which red fluorescent protein (RFP) production is controlled by a c-di-GMP-dependent riboswitch (30) (Fig. 1A). Calcium supplementation significantly increased RFP levels in biosensor-containing wild-type (WT) strain ES114 (Fig. 1B and C). This increase was dose dependent (Fig. 1B and C), indicating that increasing calcium causes an increase in intracellular c-di-GMP.

The *V. fischeri* genome contains 50 genes that encode proteins with GGDEF, EAL, or HD-GYP domains, predicted to synthesize, degrade, and/or bind c-di-GMP (31–33). To determine whether any of these genes was responsible for the calcium-dependent increase in c-di-GMP, we performed a preliminary screen evaluating biosensor activity of strains carrying single deletions of each gene. While several mutants exhibited altered responses to calcium,

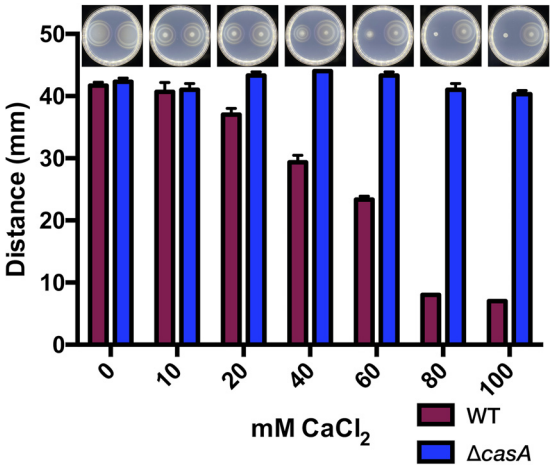


**FIG 2** CasA inhibits motility in response to calcium. Migration of WT (ES114) and the Δ*casA* mutant (KV9179) on TBS-$Mg^{2+}$ soft-agar motility plates containing increasing amounts of calcium as indicated is shown. Migration was measured as the diameter of each spot at a 4-h endpoint. Representative images (top) of each plate have WT on the left and the Δ*casA* mutant on the right. The assay was performed at least three independent times.

we report here our findings for one gene, the putative diguanylate cyclase gene *VF_1639* (Fig. 1D), which we termed *casA*, for calcium-sensing protein A. In contrast to the WT, a Δ*casA* mutant exhibited minimal changes in RFP levels up to 100 mM $CaCl_2$ (Fig. 1B and C), suggesting that CasA is critical for calcium-dependent increases in c-di-GMP.

**CasA inhibits motility in the presence of calcium.** To explore whether loss of the calcium-dependent increase in c-di-GMP in the Δ*casA* mutant translated into c-di-GMP-related phenotypes, we evaluated motility, a phenotype known to be influenced by calcium levels (25). In unsupplemented motility agar, the Δ*casA* mutant phenocopied WT migration over time (Fig. 2). In the presence of calcium, WT migration decreased in a dose-dependent manner, while migration of the Δ*casA* mutant remained constant and unaffected by concentrations up to 100 mM (Fig. 2). As migration depends on both growth and motility, we evaluated growth of the two strains to determine if differences in migration could be attributed to growth defects or advantages. In the presence of either 40 mM or 100 mM calcium, cells entered stationary phase sooner, but the WT and Δ*casA* strains were equally affected (see Fig. S1 in the supplemental material), indicating that any differences in migration are likely due to motility rather than growth. These data suggest that *V. fischeri* senses calcium and, in a manner that requires CasA, alters its migration accordingly.

**Calcium enters *V. fischeri* cells independent of CasA.** *V. fischeri* exhibits dose-dependent calcium phenotypes that are lost in a Δ*casA* mutant (Fig. 1 and 2), suggesting the possibility that a Δ*casA* mutant could be defective in calcium uptake. To evaluate if calcium enters cells, and if this uptake depends on CasA function, we expressed aequorin, a cytoplasmic photoprotein that emits light dependent on calcium binding (34, 35), in both the parent (Δ*lux*) and Δ*casA* (Δ*lux*) mutant strains. Upon exposure to 40 mM calcium, the parent strain exhibited a spike in light production, indicating that changes in exogenous calcium are reflected intracellularly (Fig. 3). The Δ*casA* strain behaved similarly to the parent strain, albeit displaying a minor decrease in activity. Thus, the inability of a *casA* mutant to respond to calcium cannot be attributed to an entry defect. Additional work will be necessary to understand the dynamics of calcium uptake; in this study, we focused on elucidating the role of CasA in the signaling network that leads to control of motility and biofilm formation.

**CasA contributes to calcium-dependent biofilm formation.** *V. fischeri* biofilms are induced by calcium (20), but it is unknown if these biofilms depend on CasA. We thus assessed biofilm formation by the WT, Δ*casA*, and complemented Δ*casA* strains grown with increasing amounts of calcium using a shaking liquid biofilm assay. In the presence of 10 mM $CaCl_2$, as previously seen (20), the WT formed a small cellulose-associated surface-adherent ring, which became more robust with increasing calcium concentrations (Fig. 4A).

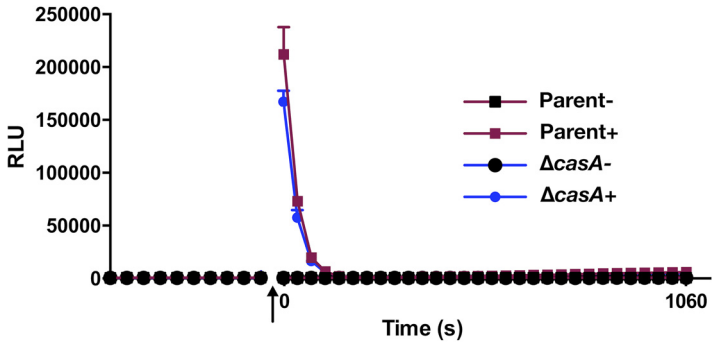


**FIG 3** Calcium uptake into bacterial cells occurs independent of CasA. Relative light units (RLU) of the Δ*luxCDABEG* (parent; EVS102) and Δ*luxCDABEG* Δ*casA* (Δ*casA*; KV9817) strains containing apoaequorin-expressing plasmid pAT103 are shown. Coelenterazine was added prior to baseline RLU (left). The arrow indicates that 40 mM calcium was added to "+" wells; "-" indicates no addition. Measurements were taken every few seconds until the endpoint. The graph is representative of at least three independent experiments.

Conversely, the Δ*casA* mutant was severely attenuated for ring formation, regardless of calcium levels. Complementation restored the Δ*casA* mutant to a WT phenotype (Fig. 4A). Quantification using crystal violet staining supported the conclusion that the Δ*casA* mutant produced significantly less adherent biomass than both the WT and complemented strains (Fig. 4B and Fig. S2A).

Because loss of CasA disrupted cellulose-dependent ring formation, we evaluated the same strains using Congo red, which can bind cellulose. On unsupplemented medium, the strains bound similar amounts of dye, resulting in streaks the same shade of red, while a cellulose mutant (Δ*bcsA*) failed to bind Congo red, resulting in yellow streaks (Fig. 4C, left). On plates with calcium, however, the Δ*casA* mutant produced yellow streaks, phenocopying the Δ*bcsA* mutant, while the WT and complemented Δ*casA* strains streaks were red (Fig. 4C, right). Quantification using ImageJ supported these visual differences (36) (Fig. S2B). Thus, *casA* is required for calcium-induced cellulose production. Additionally, while polysaccharide can decrease motility through steric hindrance (37), the Δ*bcsA* mutant migrated the same as WT, regardless of calcium (Fig. S3), suggesting that cellulose is not responsible for the calcium-mediated motility inhibition.

**CasA mediates calcium-dependent increase in *bcs* transcription.** Because calcium induces *bcs* transcription (20), we hypothesized that this effect could depend on CasA. Indeed, calcium induced significant *bcsQ* transcription in the WT but not in the Δ*casA* mutant (Fig. 5A), indicating that CasA is necessary for the calcium-dependent increase in *bcs* transcription. However, as CasA lacks DNA binding domains (Fig. 1D), it most likely acts indirectly.

VpsR was previously linked to the control of cellulose in *V. fischeri* (38); thus, we hypothesized that it regulates *bcs* transcription. Indeed, *bcsQ* transcription remained low when *vpsR* was deleted, regardless of calcium, suggesting that VpsR is necessary for *bcsQ* transcription (Fig. 5A). Complementation restored *bcsQ* transcription and the calcium-mediated increase in transcription (Fig. 5B). Thus, both *bcsQ* transcription and its induction by calcium require VpsR.

To determine if CasA was epistatic to VpsR, we overexpressed *vpsR* in a Δ*casA* Δ*vpsR* double mutant. *vpsR* overexpression increased *bcsQ* transcription but did not induce a response to calcium, indicating that CasA is needed for the calcium-dependent increase in *bcs* transcription (Fig. 5B). Additionally, *vpsR* transcription was not induced by calcium (Fig. S4A), indicating that control by calcium occurs at a different level. Of note, *vpsR* transcription was unaffected by a *casA* mutation, and it is negatively autoregulated (Fig. S4B to D). Finally, like the Δ*bcsA* mutant, the Δ*vpsR* mutant phenocopied the WT strain for motility in response to calcium (Fig. S3), further suggesting that the CasA-mediated inhibition of motility is independent of cellulose. Overall, these data suggest that VpsR is epistatic to CasA for *bcs* transcription but that the calcium-dependent increase in transcription requires CasA.

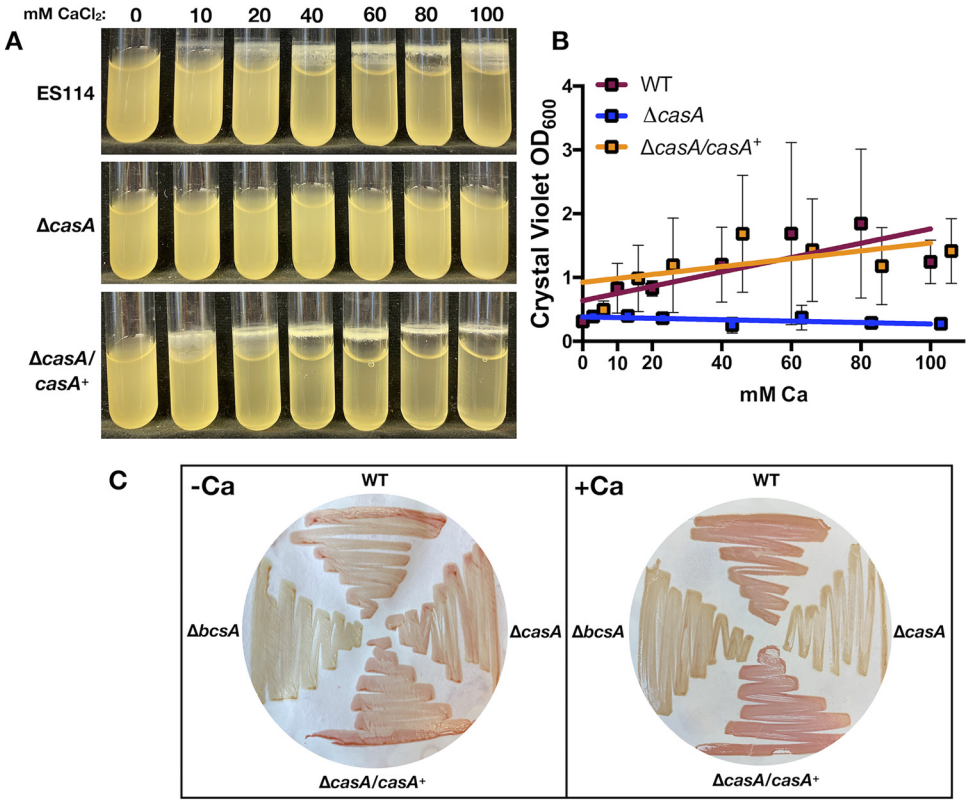


**FIG 4** CasA induces cellulose-dependent biofilms in response to calcium. (A) Shaking biofilm assay with increasing amounts of exogenous calcium added to cultures. Strains are ES114 (WT), Δ*casA* (KV9179), and Δ*casA*/*casA*$^+$ (KV9821). (B) Quantification of crystal violet staining of biofilms like those show in panel A. Symbols represent the mean of each sample and error bars show the standard deviation. Solid lines indicate linear regression analysis, where the lines that represent the WT and the Δ*casA*/*casA*$^+$ strain are not significantly different from each other but are significantly different from the Δ*casA* mutant ($P$ = 0.02). (C) Congo red dye bound to bacteria grown on LBS plates without (left) and with (right) added 40 mM calcium. Clockwise from the top, the strains are the WT (ES114) and the Δ*casA* (KV9179), Δ*casA*/*casA*$^+$ (KV9821), and Δ*bcsA* (KV7894) mutants.

**CasA is a functional DGC.** CasA contains two domains, an N-terminal periplasmic sensory domain and a C-terminal GGDEF domain (Fig. 1D), suggesting that CasA may both sense a signal(s), such as calcium, and respond accordingly by altering c-di-GMP synthesis. To probe CasA function, we evaluated complementation by hemagglutinin (HA) epitope-tagged point mutant alleles driven by a constitutive promoter and introduced into the chromosome of the Δ*casA* mutant relative to the WT-CasA-complemented strain (Δ*casA*/*casA*$^+$). All the resulting variants were produced (Fig. S5A).

First, DGC activity was evaluated by generating a G410A substitution in the second glycine of the functional GGEEF motif. c-di-GMP biosensor experiments revealed that the CasA-G410A-expressing strain phenocopied its Δ*casA* parent, failing to increase c-di-GMP levels in response to calcium (Fig. 6A and Fig. S5C). Furthermore, the CasA-G410A variant failed to complement the Congo red and motility phenotypes (Fig. 6B and C and Fig. S2C). Together, these data suggest that c-di-GMP production is necessary for the calcium-dependent biofilm and motility phenotypes controlled by CasA.

**N-terminal sensory domain controls CasA function.** The N-terminal domain of CasA contains dCache-1 (calcium and chemotaxis) and MCP-like (methyl-accepting chemotaxis protein) sensory domains, suggesting a sensory function (Fig. 1D). However, CasA lacks conserved motifs typical of such sensory domains, such as N, F, G1, G2, and G3 boxes (39, 40). Thus, to identify residues potentially important for function, we aligned CasA with homologous proteins from closely related *Vibrio* spp., via BLAST (41), and chose several highly conserved residues to mutate, with a focus on aspartates and glutamates because

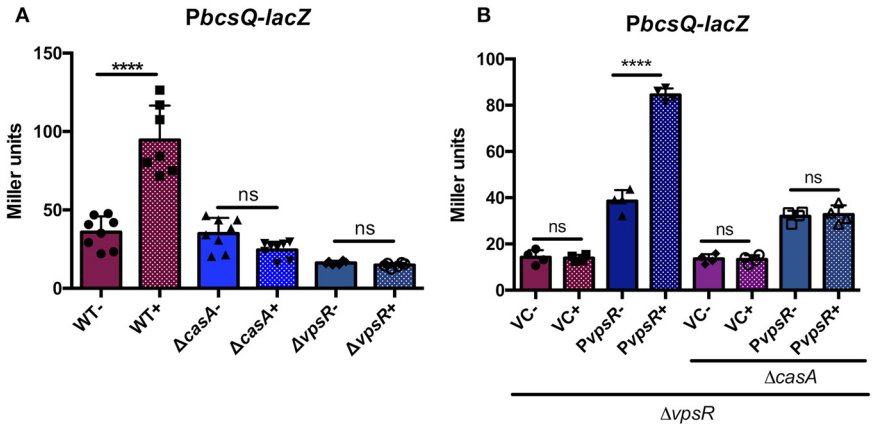


**FIG 5** Impact of calcium, CasA, and VpsR on *bcs* transcription. (A) P*bcsQ-lacZ* reporter strains WT (KV8078), Δ*casA* (KV9864), and Δ*vpsR* (KV9865) grown with (+) or without (−) 40 mM added calcium as indicated. Only the WT exhibited a significant increase in *bcsQ* transcription when calcium was added (****, $P = 0.0001$). (B) Δ*vpsR* (KV9865) single and Δ*vpsR* Δ*casA* double (KV9868) mutants containing either vector control (VC; pKV69) or *vpsR* overexpression (PvpsR; pCLD42) grown with or without 40 mM added calcium as indicated. Only a Δ*vpsR* mutant strain with pCDL42 exhibited a significant increase in transcription with calcium. Symbols represent individual values, the solid/shaded bars represent the mean of each sample, and error bars show the standard deviations. ns, not significant.

calcium is known to bind such residues: D111, G231, D236, and E293 (Fig. S6A) (42). Complementation experiments revealed two classes of phenotypes, described below.

First, one variant, CasA-D111A, exhibited increased activity while maintaining a response to calcium. Specifically, in the absence of calcium, this strain produced substantially higher levels of c-di-GMP (Fig. 7A, light blue bars, and Fig. S5D) and increased red color on Congo red (Fig. 7B and Fig. S2D). In the presence of 10 mM $CaCl_2$, this strain exhibited decreased migration compared to that of the Δ*casA*/*casA*$^+$ strain (Fig. 7C), indicating a productive response to calcium.

Second, three of the substitutions (G231A, D236A, and E293A) diminished the apparent calcium responsiveness of CasA. All three variants lost the ability to increase c-di-GMP in response to calcium and without calcium maintained similar (G231A and D236A) or slightly higher (E293A) c-di-GMP levels than the Δ*casA*/*casA*$^+$ strain (Fig. 7A and Fig. S5D). However, these variants phenocopied the Δ*casA*/*casA*$^+$ strain on Congo red agar containing calcium (Fig. 7B and Fig. S2D), indicating that they must retain some function. In support of this conclusion, they also exhibited intermediate motility phenotypes, with increased migration compared to that of the Δ*casA*/*casA*$^+$ strain but diminished migration relative to the Δ*casA* mutant at either 10 or 20 mM $CaCl_2$ (Fig. 7C). Combining the D236A and E293A substitutions resulted in a strain with slightly increased migration compared to that of each single mutant strain (Fig. S7), suggesting that this combination of substitutions decreases CasA activity but is insufficient to render CasA completely inactive. Overall, these experiments reveal four sensory domain residues that impact CasA function and calcium-dependent phenotypes, suggesting that this domain may be responsible for sensing calcium as a signal.

**CasA is sufficient for the response to calcium.** While CasA is responsible for several calcium-dependent phenotypes, it was unclear whether CasA directly senses calcium as a signal or if it requires a partner(s) to sense and respond to calcium. To explore the sufficiency of CasA in response to calcium, we used *Escherichia coli* as a heterologous system with a high-copy-number plasmid that expressed *casA*. Low calcium levels exerted minimal effects on c-di-GMP levels in *E. coli* under our conditions (Fig. 8A and B). However, when *casA* was overexpressed, addition of 10 mM calcium resulted in a significant increase in c-di-GMP (Fig. 8A and B). Furthermore, *casA*-overexpressing *E. coli* failed to migrate in soft agar when calcium was added (Fig. 8C and Fig. S8A). The vector control strain did migrate in the presence of calcium, albeit slower than in its absence, ultimately reaching the same diameter as in the absence of calcium, while the *casA*-overexpressing strain did not

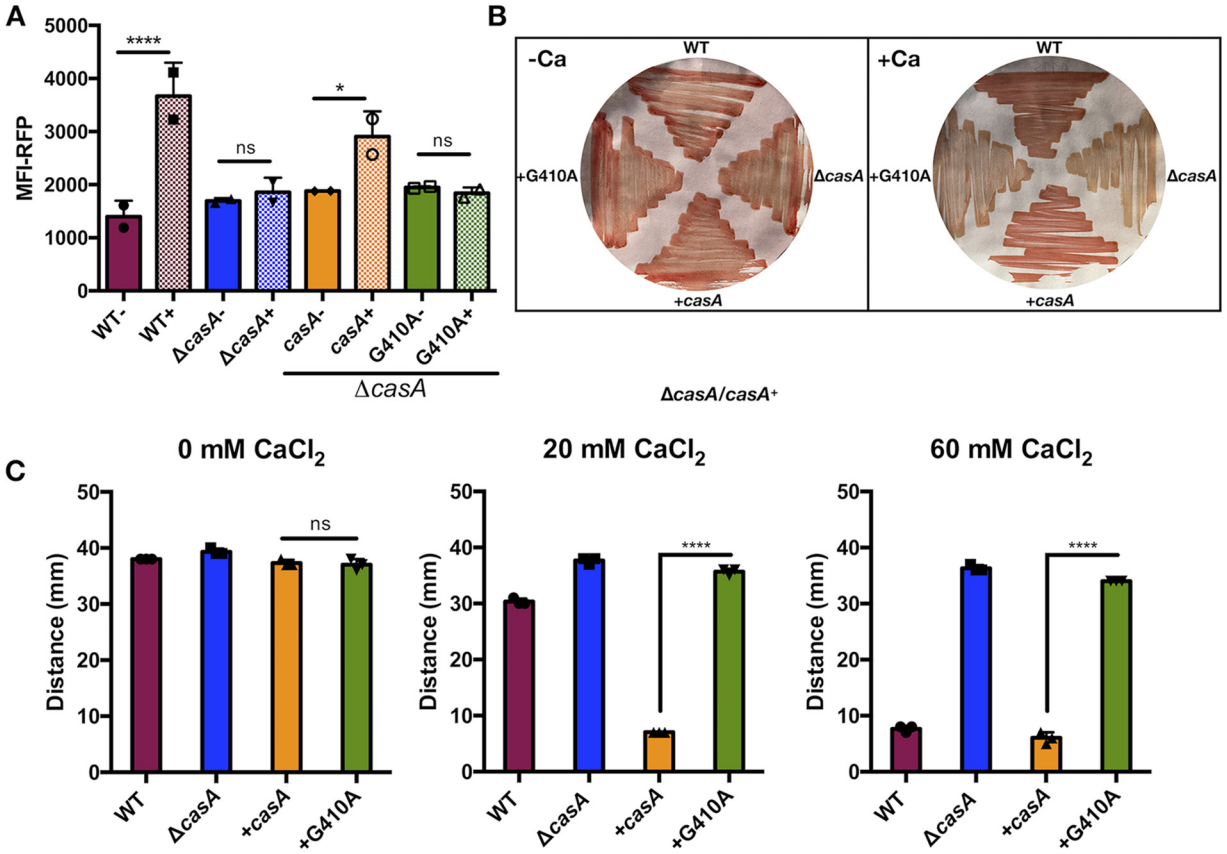


**FIG 6** Calcium-dependent phenotypes depend on CasA's enzymatic GGEEF motif. (A) MFI of RFP in AmCyan$^+$ RFP$^+$ live cells, with or without 40 mM added calcium. Only the WT and Δ*casA*/*casA*$^+$ strains increase c-di-GMP in response to calcium (****, $P = 0.0001$; *, $P = 0.01$) (B) Congo red dye bound to bacteria grown on LBS plates without (left) or with (right) 40 mM calcium. (C) Migration on motility agar containing 0, 20, or 60 mM added calcium as indicated. When calcium was added, the Δ*casA*/*casA*$^+$ strain migrated significantly less than the Δ*casA*/*casA-G410A* strain. Strains for all panels are the WT (ES114), Δ*casA* (KV9179), Δ*casA*/*casA*$^+$ (*casA*$^+$; KV9821), and Δ*casA*/*casA*-G410A (G410A; KV9822) strains. Error bars represent standard deviation. Each assay was independently performed at least three times.

progress. The calcium-induced delay in migration was not due to a growth defect (Fig. S8B). These data suggest that CasA alone is sufficient to sense calcium and inhibit motility, presumably by producing c-di-GMP.

To determine if this response (i) was dependent on the ability of CasA to make c-di-GMP and (ii) required a functional sensory domain, we evaluated the G410A enzymatic domain and D236A sensory domain variants. *E. coli* that expressed either variant phenocopied the vector control strain, with no calcium-dependent change in c-di-GMP levels or migration (Fig. 8 and Fig. S8A). These data suggest that both the periplasmic sensory domain and DGC enzymatic domain are required for CasA to sense and respond to calcium. Thus, CasA appears to be a novel calcium sensor that controls cellulose-dependent biofilm formation via a calcium-mediated induction of c-di-GMP.

**CdgK and CasA respond differently to calcium.** *V. fischeri* CasA exhibits significant homology to *V. cholerae* CdgK; when the CasA sequence was used to probe the *V. cholerae* genome by BLAST, CdgK (VC1104) was the top hit, and vice versa for CdgK and the *V. fischeri* genome (Fig. S6B). Additionally, the genes for these two proteins are immediately adjacent to a gene (encoding tRNA-dihydrouridine synthase) that is conserved in both genomes, suggesting that they could be orthologs. CdgK is one of a set of DGCs that work upstream of VpsR to activate *vps* transcription (13, 43). These similarities prompted us to explore if *cdgK* could complement the Δ*casA* mutant by expressing *cdgK* in the chromosome of a Δ*casA* mutant. This strain produced CdgK in both the presence and absence of calcium (Fig. S5B). However, it exhibited significantly decreased c-di-GMP levels in response to calcium (Fig. 9A). This suggested that CdgK is

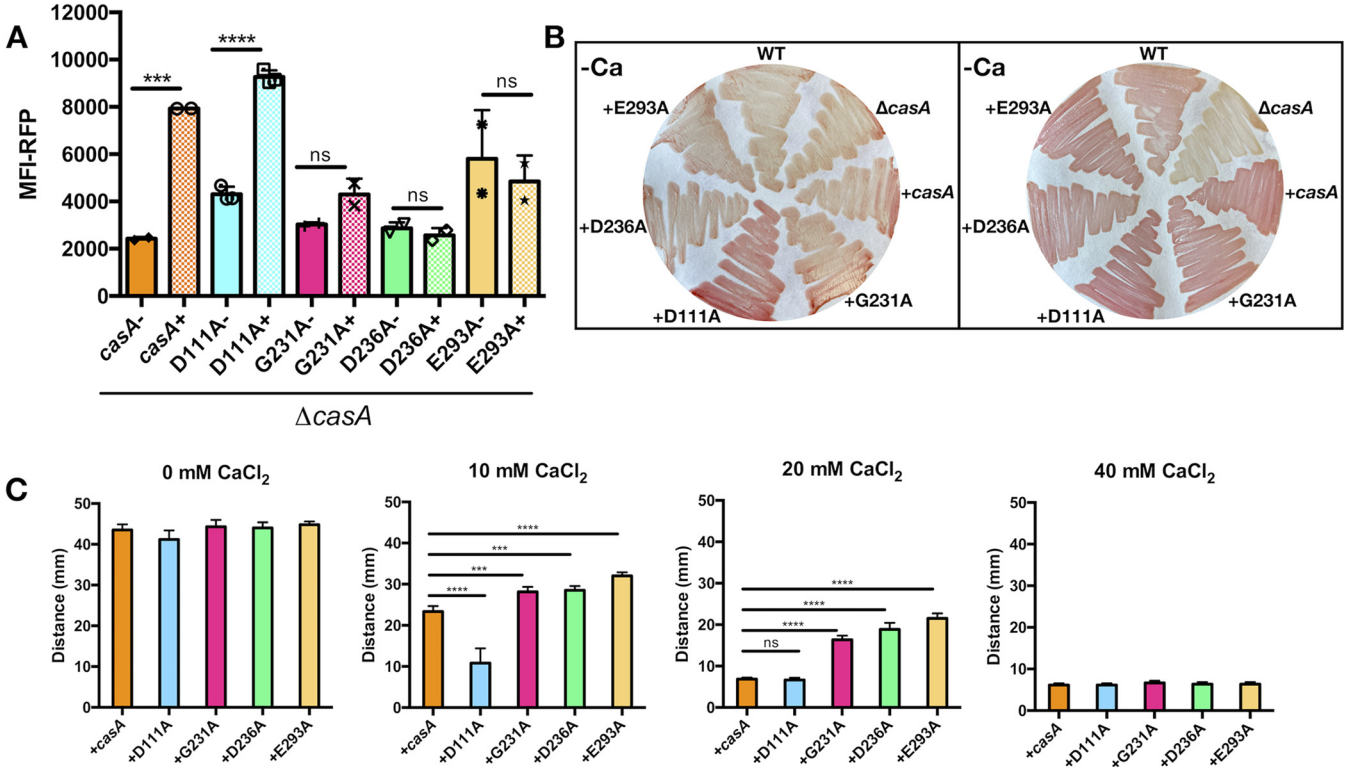


**FIG 7** Calcium-dependent phenotypes depend on CasA's N-terminal sensory domain. (A) MFI of RFP in AmCyan$^+$ RFP$^+$ live cells, with or without 40 mM added calcium. Only the Δ*casA*/*casA*$^+$ and Δ*casA*/*casA-D111A* strains increased c-di-GMP in response to calcium (***, $P$ = 0.002; ****, $P$ = 0.0001). (B) Congo red dye bound to bacteria grown on LBS plates without (left) or with (right) 40 mM calcium. (C) Migration on motility agar containing 0, 10, 20, or 40 mM calcium as indicated with an endpoint of 5 h. All variants migrated significantly differently than the parent Δ*casA*/*casA*$^+$ strain at 10 and/or 20 mM calcium addition (***, $P$ = 0.0003 to 0.0006; ****, $P$ = 0.0001). Strains for all panels are the Δ*casA*/*casA*$^+$ (*casA*$^+$; KV9821), Δ*casA*/*casA*-D111A (D111A; KV9825), Δ*casA*/*casA*-G231A (G231A; KV9824), Δ*casA*/*casA*-D236A (D236A; KV9826), and Δ*casA*/*casA*-E293A (E293A; KV9827) strains. Error bars represent standard deviation. Each assay was performed independently at least three times.

an active DGC when expressed in *V. fischeri* and that this activity may be negatively modulated by exogenous calcium. Consistent with these findings, the *cdgK*-expressing strain showed increased Congo red binding relative to controls in the absence of calcium (Fig. 9B), but with calcium supplementation, it failed to bind Congo red, phenocopying the Δ*casA* parent (Fig. 9B and Fig. S2E).

Despite the impact on c-di-GMP levels and Congo red binding, *cdgK* expression exerted no effect on motility, with or without calcium (Fig. S9). However, when we omitted the motility-promoting magnesium supplement (25), we found that it had masked the impact of *cdgK* on migration. Whereas the migration patterns of the WT, Δ*casA*, and *casA*$^+$/Δ*casA* strains mimicked those seen on plates containing magnesium (Fig. 6), the *cdgK*-expressing Δ*casA* strain behaved differently (Fig. 9C). The *cdgK*-expressing strain exhibited significantly less migration in the absence of calcium, but its migration matched that of the uncomplemented Δ*casA* parent strain when calcium was added, indicating a lack of CdgK activity under calcium conditions (Fig. 9C). Together, the observed increases in c-di-GMP levels and Congo red binding and decrease in motility of the *cdgK*-expressing strain in the absence of calcium suggest the expression of an active DGC, while the relative lack of observed activity in the presence of calcium suggests that CdgK activity may be inhibited by calcium.

## DISCUSSION

This study investigated how calcium changes *V. fischeri* behavior. We determined that increasing concentrations of calcium resulted in increased cellulose-dependent biofilm formation and decreased motility, corresponding to increasing concentrations of c-di-GMP. CasA, one of 33 putative DGCs encoded by *V. fischeri*, was solely responsible; the

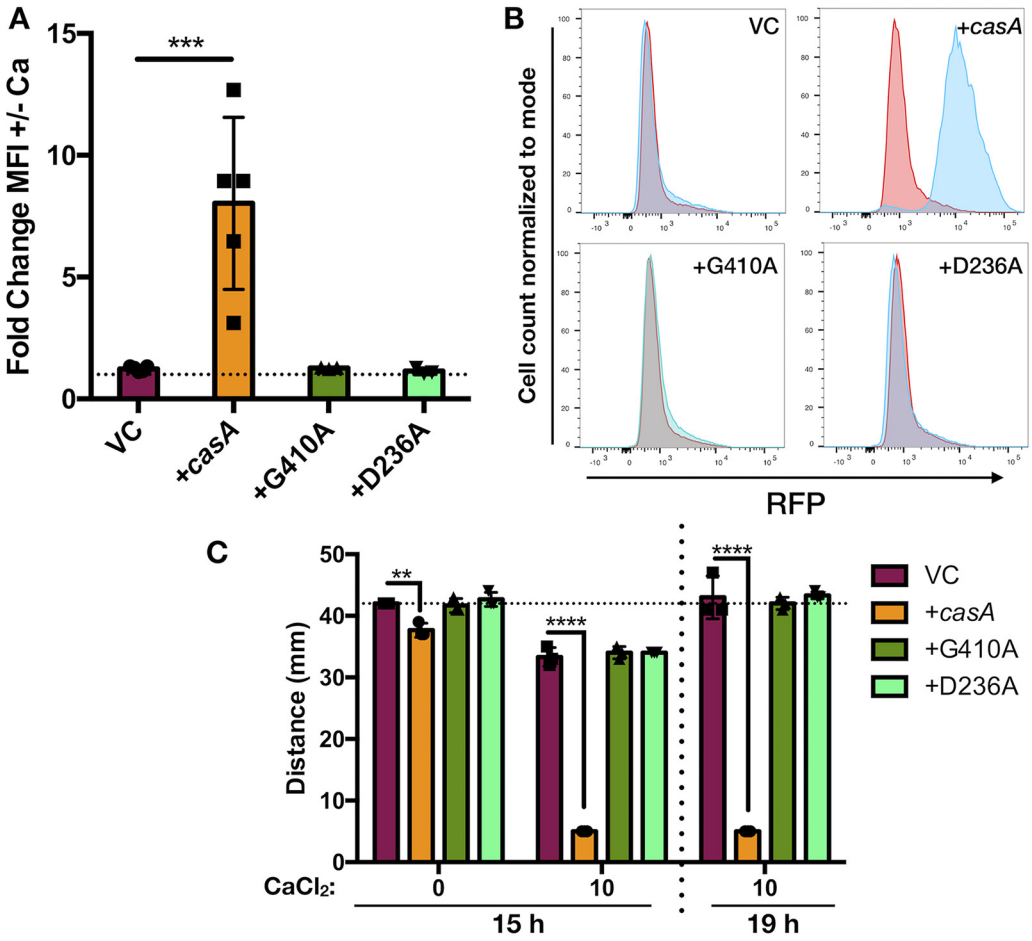


**FIG 8** Calcium activates *casA* in *E. coli*. (A) Fold change of MFI-RFP in response to 10 mM calcium in AmCyan$^+$ RFP$^+$ live cells. Overexpression of *casA* alone resulted in a significant increase in RFP in response to calcium (***, $P = 0.0006$). (B) Representative histograms of the RFP-MFI from panel A with cell count normalized to mode on the *y* axis and increasing RFP on the *x* axis. Red indicates no added calcium, and blue indicates 10 mM calcium. (C) Migration on motility agar with or without 10 mM calcium. The *y* axis represents migration distance, and the *x* axis represents added calcium. Bacteria migrate slower in the presence of calcium, independent of growth (Fig. S8B), so endpoints were chosen when the vector control (VC) reached approximately 40 mm in diameter, which was at 15 h and 19 h for 0 mM and 10 mM calcium, respectively. The horizontal dotted line represents the diameter of the VC with 0 mM calcium to facilitate a comparison of strain migration. Overexpression of *casA* resulted in significantly less migration distance relative to that of the vector control strain (**, $P = 0.003$; ****, $P = 0.0001$). Neither *casA-G410A* nor *casA-D236A* migrated significantly differently than the vector control. Strains shown contain one of the indicated plasmids: pKV69 (VC), pAT100 (*casA*), pAT101 (*casA-G410A*), pAT102 (*casA-D236A*) in *E. coli* strains GT115 (A and B), or AJW678 (C). Error bars represent standard deviation. Each assay was performed independently at least three times.

observed effects were lost in the absence of CasA, and heterologous expression of *casA* in *E. coli* similarly resulted in calcium-dependent phenotypes. For biofilm formation, the calcium-dependent increase in *bcs* transcription required both CasA and VpsR. Finally, the *V. cholerae* homolog, CdgK, did not complement CasA but instead exhibited an inverse response, with increased activity in the absence of calcium.

c-di-GMP is a widespread bacterial signal that permits many organisms to change their behavior in response to varied internal and external signals. Calcium was one of the first signals identified as an activator of c-di-GMP through inhibition of PDE activity in *Komagataeibacter xylinus*, even before the discovery of c-di-GMP in 1987 (8, 44, 45). In the intervening decades, the connection between calcium and c-di-GMP has been investigated in a variety of organisms and signaling pathways. For example, in *Mycobacterium tuberculosis*, calcium alters PDE activity, affecting growth and survival during macrophage infection (46–48). In the c-di-GMP-activated Lap systems of *Pseudomonas aeruginosa* and *Legionella pneumophila*, calcium activates the protease LapG, which promotes biofilm dispersal (49, 50).

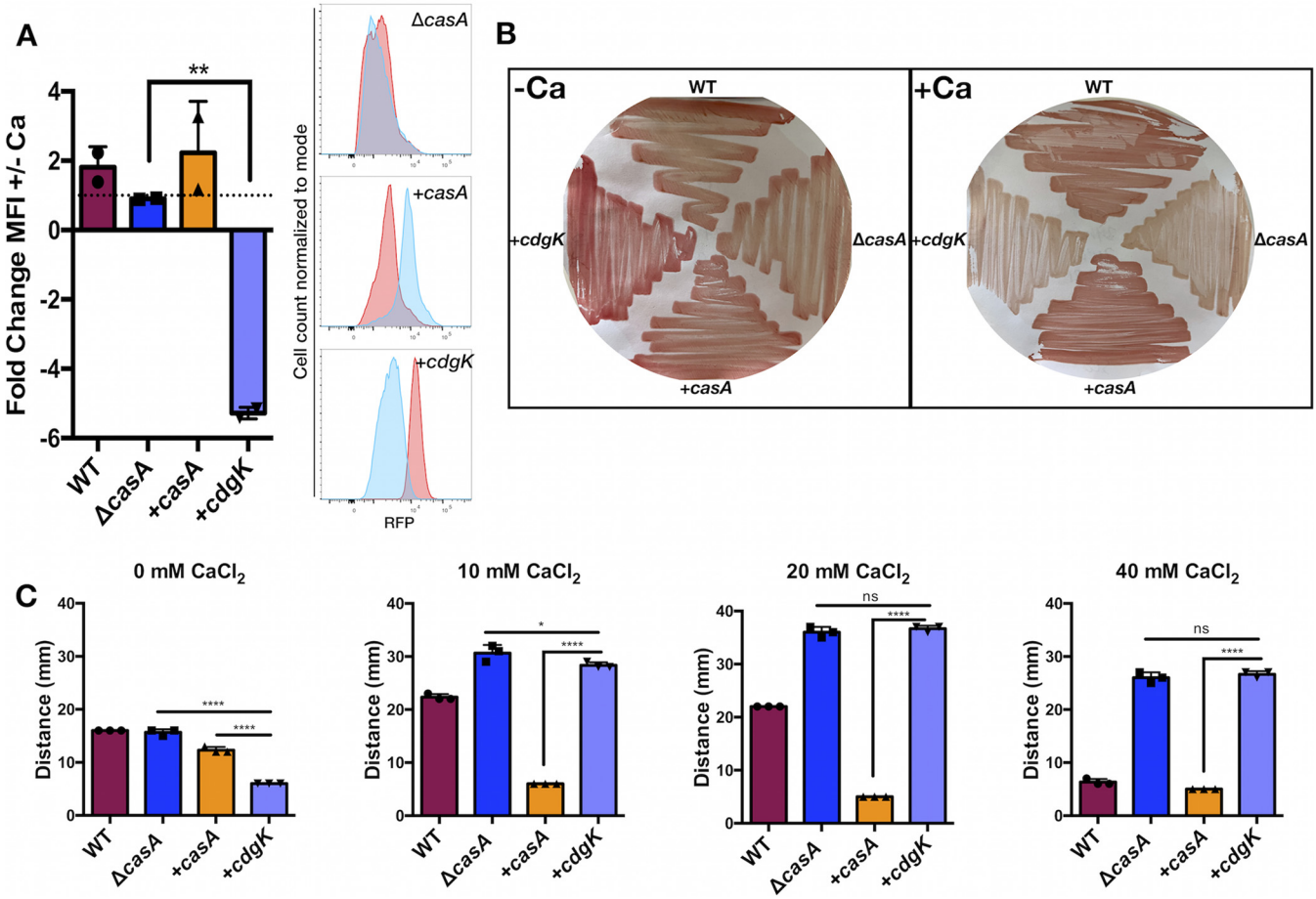


**FIG 9** *V. cholerae* CdgK calcium-dependent phenotypes. (A) Fold change of RFP-MFI (left) in response to calcium and representative histograms (right) as determined by flow cytometric analysis of AmCyan$^+$ RFP$^+$ live cells containing pFY4535. The Δ*casA*/*cdgK*$^+$ strain is significantly different from its parent Δ*casA* strain (**, $P$ = 0.0053). (B) Congo red dye bound to bacteria grown on LBS plates without (left) or with (right) 40 mM calcium. (C) Migration on motility agar containing 0, 10, 20, or 40 mM added calcium as indicated. The Δ*casA*/*cdgK*$^+$ strain is significantly different from both its parent Δ*casA* strain and the Δ*casA*/*casA*$^+$ strain in the absence of calcium (****, $P$ = 0.0001). As calcium increased, Δ*casA*/*cdgK*$^+$ migrated more similarly to the Δ*casA* strain (*, $P$ = 0.0436 at 10 mM; not significant at 20 or 40 mM) but continued to migrate significantly differently from the Δ*casA*/*casA*$^+$ strain under all calcium conditions (****, $P$ = 0.0001). Strains for all panels are the WT (ES114), Δ*casA* (KV9179), Δ*casA*/*casA*$^+$ (KV9821), and Δ*casA*/*cdgK*$^+$ (KV9828) strains. Error bars represent standard deviation. Each assay was performed independently at least three times.

Additionally, similar to what we observed in this study, calcium increases intracellular c-di-GMP levels in *V. vulnificus* (19). Our work adds to this literature by identifying CasA as a DGC whose activity is induced in response to calcium. Other DGCs and PDEs responsive to calcium in a variety of organisms are likely to be uncovered as the connection between calcium and c-di-GMP continues to be explored.

The architecture of CasA includes a putative N-terminal periplasmic sensory domain—putatively involved in binding calcium—and a well-conserved C-terminal cytoplasmic GGDEF enzymatic domain responsible for c-di-GMP production. Residues in both of these domains are required for function. Protein prediction programs identify both dCache-1 (calcium and chemotaxis) and MCP-like (methyl-accepting chemotaxis protein) domains in the N terminus. Class I MCPs have a periplasmic ligand binding domain (LBD), with another, functional domain in the cytoplasm (51), matching the general structure of CasA. A screen of calcium-binding proteins identified aspartates and glutamates as the most common calcium-coordinating residues (42). Consistent with those known interactions, N-terminal CasA residues D236 and E293 likely contribute to sensing/binding calcium in some way, as mutating these residues resulted in partial loss of the calcium response. Conversely, mutation of D111 allowed for an increase in basal CasA function without disrupting the ability to sense/respond to calcium. Structural analysis of CasA could provide insight into where and how calcium binds to the N-terminal LBD.

CasA responds to the calcium signal by synthesizing c-di-GMP to control cellulose production. A wide variety of bacterial species synthesize cellulose polysaccharide, leading to a diversity of *bcs* operon structures, genes, cellulose products, and regulatory mechanisms. But throughout this heterogeneity, bacterial cellulose remains inextricably linked to c-di-GMP, as all identified BCS complexes contain a BcsA subunit with a PilZ c-di-GMP binding domain (52). *E. coli* and *Salmonella* spp. are the best-studied organisms with type II *bcs* operons, the same kind found in *V. fischeri*. In *V. fischeri*, regulation starts at the transcriptional level, where *bcs* transcription depends on VpsR and is significantly increased by calcium due to the DGC CasA. Without CasA, calcium has no impact on either the internal levels of c-di-GMP or *bcs* transcription. Conversely, in *E. coli* and *Salmonella* spp., *bcs* transcription is thought to be constitutively active and therefore unregulated (53). However, posttranscription regulation of cellulose by c-di-GMP is well established in these organisms, with c-di-GMP binding to and allosterically activating BcsA promoting synthesis and binding to BcsE, activating BcsG for postsynthetic modification (54, 55). While this has not yet been investigated, c-di-GMP almost certainly regulates cellulose synthesis in *V. fischeri* by binding to and activating the predicted BcsA and BcsE proteins, perhaps due to CasA-relayed calcium and/or additional signals. The PDE BinA is known to impact cellulose polysaccharide and represents another candidate for cellulose regulation at the synthesis or postsynthetic level (56).

Regulation of the *bcs* locus in *V. fischeri* contains parallels to regulation of other *Vibrio* polysaccharide loci and is often directly inverse to regulation in *V. cholerae*. First, calcium affects transcription of a major polysaccharide locus in at least three different *Vibrio* spp., activating *bcs* and *brp* transcription in *V. fischeri* and *V. vulnificus*, respectively, and downregulating *vps* transcription in *V. cholerae* (18–20). Calcium acts to increase c-di-GMP in both *V. fischeri* and *V. vulnificus*, activating CasA in *V. fischeri* to increase *bcs* transcription (19). The specific calcium-dependent mechanism activating *brp* transcription is yet unknown but also dependent on c-di-GMP (19). Conversely, in *V. cholerae*, *vps* transcription is decreased by calcium through downregulation of *vpsR* transcription by the calcium-sensing two-component system CarRS (18). Second, the homologous transcriptional regulators VpsR in both *V. fischeri* and *V. cholerae* autoregulate their own transcription, albeit in opposite directions, with *V. fischeri* VpsR negatively autoregulating and *V. cholerae* VpsR engaging in positive autoregulation (57). Third, the homologous DGCs CasA and CdgK respond oppositely to calcium, with CasA increasing and CdgK decreasing c-di-GMP levels in the presence of calcium, paralleling the effects on *bcs* and *vps* transcription. In *V. cholerae*, VpsR activity is increased by c-di-GMP (11, 12). This is likely to be the case for the *V. fischeri* protein as well; if so, this could account for CasA-mediated induction of *bcs* transcription in response to calcium. Overall, these differences in regulation speak to the evolutionary divergence between species, with the same signal allowing each organism to adapt to its environmental niches without major functional changes.

In summary, this study identifies CasA as a calcium-sensing DGC in *V. fischeri*, responsible for inducing cellulose-dependent biofilm formation and inhibiting motility in response to calcium. CasA is required for a calcium-dependent increase in *bcs* transcription, connecting c-di-GMP to transcriptional control of a type II *bcs* locus. The *V. cholerae* homolog, CdgK, and CasA are not equivalent, but the enzymatic activity of both proteins seems to be modulated by calcium, providing insight into how related species can adapt to their specific niches.

## MATERIALS AND METHODS

**Strains and media.** *V. fischeri* strains, plasmids and primers used in this study are listed in Tables 1 to 3. All strains used in this study were derived from strain ES114, a bacterial isolate from *Euprymna scolopes* (58). *Escherichia coli* strains TAM1 (Active Motif), TAM1 $\lambda$ *pir* (Active Motif), DH5$\alpha$, $\pi$3813, and GT115 were used for cloning (59). For routine culturing, *V. fischeri* strains were grown in LBS (60, 61) and *E. coli* strains were grown in LB (62), in some cases supplemented with thymidine. For natural transformation of *V. fischeri*, Tris minimal medium (TMM) (100 mM Tris [pH 7.5], 300 mM NaCl, 0.1% ammonium chloride, 10 mM *N*-acetylglucosamine, 50 mM $MgSO_4$, 10 mM KCl, 10 mM $CaCl_2$, 0.0058% $K_2HPO_4$, 10 $\mu$M ferrous ammonium sulfate) was used. Soft-agar motility medium (tryptone broth [TB] for *E. coli* and tryptone broth salt [TBS] for *V. fischeri*) contained tryptone (1%), NaCl (2% for *V. fischeri* and 1% for *E. coli*), agar (0.25%), and $MgSO_4$ (35 mM), and $CaCl_2$ was added to the desired concentration. Antibiotics were added as appropriate at the following final concentrations: ampicillin (Amp), 100 $\mu$g ml$^{-1}$; chloramphenicol (Cm),

**TABLE 1** Strains used in this study

| Strain | Genotype[a] | Construction[b] | Reference |
|---|---|---|---|
| AJW678 | *thi-1 thr-1*(Am) *leuB6 metF159*(Am) *rpsL136* Δ*lacX74* | | 75 |
| ES114 | WT | | 58 |
| EVS102 | Δ*luxCDABEG* | | 76 |
| KV7371 | IG::P*sypA-lacZ* | | 77 |
| KV7894 | Δ*bcsA* | | 20 |
| KV8078 | Δ*sypQ*::FRT-Cm$^r$ attTn*7*::P*bcsQ-lacZ* | | 20 |
| KV8232 | IG (*yeiR-glmS*)::Erm$^r$-trunc Trim$^r$ | | 68 |
| KV8920 | Δ*casA*::FRT-Spec$^r$ | TT ES114 via intermediate strain generated with SOE using primers 2561 and 2562 (ES114), 2089 and 2090 (pKV521), and 2563 and 2564 (ES114) | This study |
| KV9179 | Δ*casA*::FRT | KV8920 with Spec$^r$ cassette removed using pKV496 | This study |
| KV9341 | Δ*vpsR*::FRT-Spec$^r$ | TT ES114 with SOE using primers 2093 and 2094 (ES114), 2089 and 2090 (pKV521), and 2095 and 2096 (ES114) | This study |
| KV9573 | IG::P*vpsR-lacZ* | TT KV7371 with SOE using primers 2185 and 2090 (pKV502), 2932 and 2933 (ES114), and 2822 and 2876 (KV7371); replaces P*sypA-lacZ* | This study |
| KV9807 | Δ*casA*::FRT-Spec$^r$ IG::P*nrdR-casA-D236A-E293A*-HA | TT KV9818 with SOE using primers 2290 and 3122 (KV9826) and 3121 and 1487 (KV9827) | This study |
| KV9817 | Δ*luxCDABEG* Δ*casA*::FRT-Spec$^r$ | TT EVS102 with gKV9821 | This study |
| KV9818 | Δ*casA*::FRT-Spec$^r$ IG::Erm$^r$-trunc Trim$^r$ | TT KV8232 with gKV8920 | This study |
| KV9820 | Δ*casA*::FRT-Spec$^r$ IG::P*nrdR-casA*-HA | TT KV9818 with SOE using primers 2290 and 2090 (pKV506), 2905 and 3042(ES114), and 2089 and 1487 (pKV505) | This study |
| KV9821 | Δ*casA*::FRT-Spec$^r$ IG::P*nrdR*-RBS-*casA*-HA | TT KV9818 with SOE using primers 2290 and 2090 (pKV506) and 3057 and 1487 (KV9820) | This study |
| KV9822 | Δ*casA*::FRT-Spec$^r$ IG::P*nrdR*-RBS-*casA-G410A*-HA | TT KV9818 with SOE using primers 2290 and 2911 (KV9821) and 2910 and 1487 (KV9821) | This study |
| KV9824 | Δ*casA*::FRT-Spec$^r$ IG::P*nrdR*-RBS-*casA-G231A*-HA | TT KV9818 with SOE using primers 2290 and 3112 (KV9821) and 3111 and 1487 (KV9821) | This study |
| KV9825 | Δ*casA*::FRT-Spec$^r$ IG::P*nrdR*-RBS-*casA-D111A*-HA | TT KV9818 with SOE using primers 2290 and 3118 (KV9821) and 3117 and 1487 (KV9821) | This study |
| KV9826 | Δ*casA*::FRT-Spec$^r$ IG::P*nrdR*-RBS-*casA-D236A*-HA | TT KV9818 with SOE using primers 2290 and 3120 (KV9821) and 3119 and 1487 (KV9821) | This study |
| KV9827 | Δ*casA*::FRT-Spec$^r$ IG::P*nrdR*-RBS-*casA-E293A*-HA | TT KV9818 with SOE using primers 2290 and 3122 (KV9821) and 3121 and 1487 (KV9821) | This study |
| KV9828 | Δ*casA*::FRT-Spec$^r$ IG::P*nrdR*-RBS-*cdgK*-HA | TT KV9818 with SOE using primers 2290 and 2090 (pKV506), *cdgK* gblock (IDT), and 2089 and 1487 (pKV505) | This study |
| KV9864 | Δ*sypQ*::FRT-Cm$^r$ Δ*casA*::FRT-Spec$^r$ attTn*7*::P*bcsQ-lacZ* | TT KV8078 with gKV8920 | This study |
| KV9865 | Δ*sypQ*::FRT-Cm$^r$ Δ*vpsR*::FRT-Spec$^r$ attTn*7*::P*bcsQ-lacZ* | TT KV8078 with gKV9341 | This study |
| KV9866 | Δ*casA*::FRT Δ*vpsR*::FRT-Spec$^r$ | TT KV9179 with gKV9341 | This study |
| KV9867 | Δ*vpsR*::FRT-Spec$^r$ IG::P*vpsR-lacZ* | TT KV9573 with gKV9341 | This study |
| KV9868 | Δ*casA*::FRT Δ*vpsR*::FRT-Spec$^r$ attTn*7*::P*bcsQ-lacZ* | Derived from KV9866 using pCMA26 (20) | This study |
| KV9929 | Δ*casA*::FRT-Spec$^r$ IG::P*vpsR-lacZ* | TT KV9573 with gKV8920 | This study |

[a]Abbreviations: HA, HA epitope tagged; IG, intergenic between *yeiR* and *glmS* (adjacent to the Tn*7* site); FRT, the antibiotic cassette was resolved using Flp recombinase, leaving a single FRT sequence.

[b]Derivation of strains constructed in this study. TT, TfoX-mediated transformation of a *tfoX*-overexpressing version of the indicated strain with the indicated genomic DNA (gDNA) or with a PCR-SOE product generated using the indicated primers and templates.

1 $\mu$g ml$^{-1}$; erythromycin (Em), 2.5 $\mu$g ml$^{-1}$ (*V. fischeri*) or 150 $\mu$g ml$^{-1}$ (*E. coli*); kanamycin (Kn), 100 $\mu$g ml$^{-1}$ (*V. fischeri*) or 50 $\mu$g ml$^{-1}$ (*E. coli*); spectinomycin (Sp), 200 $\mu$g ml$^{-1}$; and gentamicin (Gen), 5 $\mu$g ml$^{-1}$. For Sp and Gen, LB was used as the medium instead of LBS for outgrowth and plating.

**Molecular techniques and strain construction.** Mutations in ES114 were generated through TfoX-mediated transformation (63–66). Briefly, ~500-bp segments upstream and downstream of genes of interest were PCR amplified using high-fidelity KOD polymerase (Novagen, EMD Millipore), and PCR splicing by overlap extension (SOE [67]) was used to fuse segments to an antibiotic cassette as described previously (68). The fused product was amplified and transformed into the recipient *V.*

**TABLE 2** Plasmids used in this study

| Name | Description | Derivation[a] | Reference |
|---|---|---|---|
| pAT100 | pJET + FRT-Erm$^r$ *casA*-HA | pJET + PCR product with primers 975 and 1487 (KV9821) | This study |
| pAT101 | pJET + FRT-Erm$^r$ *casA*+*G410A*-HA | pJET + PCR product with primers 975 and 1487 (KV9822) | This study |
| pAT102 | pJET + FRT-Erm$^r$ *casA*+*D236A*-HA | pJET + PCR product with primers 975 and 1487 (KV9826) | This study |
| pAT103 | Apoaequorin, Cm$^r$ | pVSV105 + apoaequorin | This study |
| pCLD42 | pKV69 + *vpsR* | | 38 |
| pCMA26 | P*bcsQ-lacZ* reporter | | 20 |
| pFY4535 | c-di-GMP biosensor; Gen$^r$ *hok*/*sok* | | 30 |
| pJJC4 | *tfoX*$^+$ + Cm$^r$ | | 66 |
| pKV69 | Vector; Cm$^r$ Tet$^r$ | | 78 |
| pKV496 | Kan$^r$ + *flp*$^+$ | | 68 |
| pKV502 | pJET + *yeiR*-FRT-Erm$^r$ | | 68 |
| pKV505 | pJET + HA-*glmS* | | 68 |
| pKV506 | pJET + yeiR-FRT-Erm$^r$-P*nrdR* | | 68 |
| pKV521 | pJET + FRT-Spec$^r$ | | 68 |
| plostfoX-Kan | *tfoX*$^+$ + Kan$^r$ | | 64 |
| pVSV105 | Vector; Cm$^r$ | | 73 |

[a]Derivation of plasmids generated in this study.

*fischeri* strain (typically ES114) carrying a TfoX-overproducing plasmid (plostfoX [64], plostfoX-Kan [64], or pJJC4 [66]), and recombinant cells were selected on media containing the appropriate antibiotic. The allelic replacement was confirmed by PCR with outside primers using Promega *Taq* polymerase (Table 3). After the initial deletion was made, genomic DNA (gDNA) was isolated from the recombinant strains using the Quick-DNA Miniprep plus kit (Zymo Research) and used to introduce the mutation into other desired strain backgrounds. Insertion at the Tn*7* site was performed via tetraparental mating (69) between the *V. fischeri* recipient and three *E. coli* strains, carrying the conjugal plasmid pEVS104 (70), the Tn*7* transposase plasmid pUX-BF13 (71), and pCMA26 (20). Insertions were also introduced adjacent to the Tn*7* site at the intergenic (IG) region between *yeiR* and *glmS* as previously described (68). These insertions were

**TABLE 3** Primers used in this study

| Primer no. | Sequence[a] |
|---|---|
| 975 | CCTCACCCCAGATGGTTTGGCA |
| 1487 | GGTCGTGGGGAGTTTTATCC |
| 2089 | CCATACTTAGTGCGGCCGCCTA |
| 2090 | CCATGGCCTTCTAGGCCTATCC |
| 2093 | ATCACAGCTCTTGAGCATGG |
| 2094 | TAGGCGGCCGCACTAAGTATGGTTGAGTACCCATAACACTACCTC |
| 2095 | GGATAGGCCTAGAAGGCCATGGAGCTATAGCTAATCGAATCCTTATTG |
| 2096 | CTGGCAGTAAACCTTTACCTG |
| 2185 | CTTGATTTATACAGCGAAGGAG |
| 2290 | AAGAAACCGATACCGTTTACG |
| 2561 | GCGCAGCAATTGATTACAGC |
| 2562 | taggcggccgcactaagtatggCAACACTAGGAATAGTGTTGG |
| 2563 | ggataggcctagaaggccatggGGTAAAAACCGAGTTTACTTTTC |
| 2564 | CTAACCATTCATGCAAGAACC |
| 2822 | AGGAAACAGCTatgACCATGATTACGGATTCAC |
| 2876 | GAAACGCCGAGTTAACGCC |
| 2905 | ggataggcctagaaggccatggCACTTCGTGTTAAAGAATTTATAC |
| 2910 | CGATTTGGCGCTGAAGAATTTGTTATCTGTATTAATG |
| 2911 | CAAATTCTTCAGCGCCAAATCGAGACACAATATC |
| 2932 | ggataggcctagaaggccatggCCATCAATGCGTCCACAAGC |
| 2933 | catggtcatagctgtttcctCATAACACTACCTCTAAATTCTTATATC |
| 3042 | ttatgcataatctggaacatcatatggataTGAAAAGTAAACTCGGTTTTTACC |
| 3057 | ggataggcctagaaggccatggAGGAGGATTTATACATGCCGAAATTTAATTTAAAAC |
| 3111 | GTATATTCAAAGCTGTATTGGTCATTGATCTTTC |
| 3112 | GACCAATACAGCTTTGAATATACCTTTATAG |
| 3117 | GGACGTCTTGCTTATAGTATCGCTGGTAAAAAAG |
| 3118 | GATACTATAAGCAAGACGTCCTTCTGCAAC |
| 3119 | GTATTGGTCATTGCTCTTTCAGTTGAAAAGC |
| 3120 | CTGAAAGAGCAATGACCAATACACCTTTG |
| 3121 | GATAAAAGAAGCGTTGAAAGGTTTTCTTGTG |
| 3122 | CTTTCAACGCTTCTTTTATCGATGTTTTG |

[a]Lowercase letters indicate nonnative or tail sequences.

made using the PCR amplification and SOE method described above, with genes of interest fused to an upstream Erm$^r$ cassette for selection, driven by the constitutive P*ndrR* promoter, and containing an idealized ribosome binding site (RBS). In some cases, the antibiotic resistance cassette was removed from *V. fischeri* deletion mutants using Flp recombinase, which acts on Flp recombination target (FRT) sequences to delete the intervening sequences, as has previously been shown (72). Overexpression plasmids were constructed by amplifying genes of interest from the IG region of *V. fischeri* strains, and the resulting PCR product was ligated into the pJET1.2 blunt cloning vector (Thermo Fisher), transformed into chemically competent *E. coli* DH5$\alpha$, and selected using Amp. The resulting plasmids were sequenced (Integrated DNA Technologies), purified using the plasmid miniprep kit (Zymo Research), and transformed into chemically competent *E. coli* FT115 containing either the pFY4535 biosensor or AJW678. The apoaequorin plasmid was synthesized by GenScript using sequence from *Aequorea victoria* for apoaequorin, clone UTAEQ04, and inserted into plasmid pVSV105 (73).

**c-di-GMP biosensor assay.** Relative c-di-GMP levels were assessed in either LBS or LB broth at 24 or 28°C for *V. fischeri* and *E. coli*, respectively, and cultures inoculated from single colonies contained added calcium chloride as indicated. The biosensor was not selected using antibiotics, as it contains a toxin/antitoxin system (30), but Amp was used to select for overexpression plasmids in *E. coli* strains. Samples were diluted 1:1,000 in phosphate-buffered saline (PBS) and assessed via flow cytometry on a LSRFortessa (BD Biosciences). Forward scatter (FSC) and side scatter (SSC) were collected in a log scale with a threshold of 200, and AmCyan and phycoerythrin (PE)-Texas Red channels were used to measure AmCyan and RFP, respectively. Data were analyzed using FlowJo 10, gating first on live cells as determined by FSC and SSC, then AmCyan to confirm singlets, and finally RFP to assess relative c-di-GMP. This resulting population was used to create representative histograms, and the geometric mean fluorescence intensity (MFI) of each curve was used to quantify and compare samples. Data were graphed using GraphPad Prism 6 and analyzed via linear regression or one-way analysis of variance (ANOVA) as indicated.

**Aequorin assay.** The Δ*luxCDABEG* strain (parent) and its Δ*casA* derivative carrying pAT103 were grown overnight at 28°C in LBS with Cm. The overnight cultures were subcultured 1:100, grown until mid-log phase, and collected and centrifuged. Samples were washed two times and resuspended in PBS, and a limiting amount of coelenterazine (Nanolight Technology) was added to a final concentration of 5 $\mu$M. The samples were vortexed and incubated in the dark for 1 h and washed in PBS, and the optical density at 600 nm ($OD_{600}$) was measured. Samples were normalized to an OD of 0.4 in a white 96-well plate and incubated in the dark for 10 min. The baseline luminescence of the samples was measured with a delay of 1 s for 5.9 min in a luminometer (Veritas microplate luminometer; Turner Biosystems). Calcium was added to a final concentration of 40 mM, and the luciferase activity was measured with a delay of 1 s for approximately 17 min 40 s. The limiting amount of coelenterazine is responsible for the temporal appearance of light production. This assay was performed at least three separate times.

**Motility assay.** Single colonies were inoculated in either TBS or TB for *V. fischeri* and *E. coli*, respectively. Cultures were grown overnight shaking at 28°C, subcultured 1:100 in fresh broth, and incubated with shaking until exponential growth phase. Cultures were normalized to a final $OD_{600}$ of 0.2, and 10-$\mu$l aliquots were spotted onto soft-agar motility plates supplemented with the desired concentrations of $CaCl_2$. *E. coli* plasmids were maintained with Amp throughout. Plates were incubated at 28°C, and the diameter of each zone of migration was measured and imaged at 4 h unless indicated otherwise for *V. fischeri* and 15 h and 19 h for *E. coli*. Pictures were taken using an iPhone 11 front-facing camera. Data were analyzed using one-way ANOVA in GraphPad Prism 6. Each experiment utilizing this assay was performed at least three independent times.

**Shaking biofilm assay.** To assess calcium-induced biofilm formation under shaking liquid conditions, LBS broth containing between 10 and 100 mM calcium chloride (as indicated) was inoculated with single colonies of *V. fischeri* strains and grown with shaking overnight at 24°C. For these experiments only, test tubes (13 by 100 mm) were used with a culture volume of 2 ml of LBS broth. For crystal violet staining, 200 $\mu$l of a 1% crystal violet solution was added to cultures for 30 min. Tubes were washed with deionized $H_2O$ and destained with ethanol. $OD_{600}$ was measured using a Synergy H1 microplate reader (BioTek). Pictures were captured via an iPhone 12 minicamera, and data are representative of at least 3 independent experiments. Linear regression analysis was performed in GraphPad Prism 6.

**Congo red assay.** Bacteria were streaked onto LBS plates containing Congo red and Coomassie blue dyes (40 $\mu$g ml$^{-1}$ and 15 $\mu$g ml$^{-1}$, respectively), and 40 mM calcium as indicated, and grown overnight at 24°C. To better visualize color differences, cells were transferred onto white paper in a replica plating-like approach by briefly smoothing the paper onto the agar plate and then lifting it off (68). The result was photographed with an iPhone 12 minicamera. For quantification, 10-$\mu$l aliquots of culture normalized to an OD of 0.2 were spotted and grown as described above. Spots were compared by assessing the gray values via ImageJ (36).

**$\beta$-Galactosidase assay.** Strains carrying a *lacZ* reporter fusion to the *bcsQ* or *vpsR* promoter were grown in duplicate at 24°C in LBS containing calcium chloride as indicated. Strains were subcultured into 20 ml of fresh medium in 125-ml baffled flasks, and samples were collected after 4 h of growth. $OD_{600}$ was measured, and cells were resuspended in Z buffer and lysed with chloroform. The $\beta$-galactosidase activity of each sample was assayed as described previously (74) and measured using a Synergy H1 microplate reader (BioTek). Assays were performed at least 2 independent times and analyzed via one-way ANOVA in GraphPad Prism 6.

## SUPPLEMENTAL MATERIAL

Supplemental material is available online only.

**TEXT S1**, PDF file, 0.1 MB.

**FIG S1**, PDF file, 0.04 MB.

**FIG S2**, PDF file, 0.4 MB.
**FIG S3**, PDF file, 0.04 MB.
**FIG S4**, PDF file, 0.1 MB.
**FIG S5**, PDF file, 0.1 MB.
**FIG S6**, PDF file, 0.04 MB.
**FIG S7**, PDF file, 0.1 MB.
**FIG S8**, PDF file, 0.1 MB.
**FIG S9**, PDF file, 0.04 MB.

## ACKNOWLEDGMENTS

We thank Ali Razvi, Cindy Darnell, and Steven Eichinger for strain construction, Fitnat Yildiz for generously sharing pFY4525, Pat Simms and the Iwashima lab for help with flow cytometry and analysis, members of our lab and the Stabb lab for thoughtful discussion, and Courtney Dial for review of the manuscript.

This work was supported by the Schmitt Fellowship awarded to A.H.T. and NIH grant GM130355 awarded to K.L.V.

A.H.T. contributed to conceptualization, formal analysis, funding acquisition, investigation, methodology, project administration, supervision, visualization, validation, and writing - original draft, review, and editing. M.E.V. contributed to investigation, visualization, and writing - review. N.P. contributed to investigation, methodology, and writing - review. K.L.V. contributed to conceptualization, funding acquisition, methodology, project administration, resources, supervision, validation, and writing - original draft, review, and editing.

## REFERENCES

1. Flemming HC, Wingender J. 2010. The biofilm matrix. Nat Rev Microbiol 8:623–633. https://doi.org/10.1038/nrmicro2415.
2. Dragoš A, Kovács Á T. 2017. The peculiar functions of the bacterial extracellular matrix. Trends Microbiol 25:257–266. https://doi.org/10.1016/j.tim.2016.12.010.
3. Römling U, Galperin MY, Gomelsky M. 2013. Cyclic di-GMP: the first 25 years of a universal bacterial second messenger. Microbiol Mol Biol Rev 77:1–52. https://doi.org/10.1128/MMBR.00043-12.
4. Valentini M, Filloux A. 2016. Biofilms and cyclic di-GMP (c-di-GMP) signaling: lessons from Pseudomonas aeruginosa and other bacteria. J Biol Chem 291:12547–12555. https://doi.org/10.1074/jbc.R115.711507.
5. Hecht GB, Newton A. 1995. Identification of a novel response regulator required for the swarmer-to-stalked-cell transition in Caulobacter crescentus. J Bacteriol 177:6223–6229. https://doi.org/10.1128/jb.177.21.6223-6229.1995.
6. Galperin MY, Natale DA, Aravind L, Koonin EV. 1999. A specialized version of the HD hydrolase domain implicated in signal transduction. J Mol Microbiol Biotechnol 1:303–305.
7. Tal R, Wong HC, Calhoon R, Gelfand D, Fear AL, Volman G, Mayer R, Ross P, Amikam D, Weinhouse H, Cohen A, Sapir S, Ohana P, Benziman M. 1998. Three cdg operons control cellular turnover of cyclic di-GMP in Acetobacter xylinum: genetic organization and occurrence of conserved domains in isoenzymes. J Bacteriol 180:4416–4425. https://doi.org/10.1128/JB.180.17.4416-4425.1998.
8. Ross P, Weinhouse H, Aloni Y, Michaeli D, Weinberger-Ohana P, Mayer R, Braun S, de Vroom E, van der Marel GA, van Boom JH, Benziman M. 1987. Regulation of cellulose synthesis in *Acetobacter xylinum* by cyclic diguanylic acid. Nature 325:279–281. https://doi.org/10.1038/325279a0.
9. Conner JG, Zamorano-Sanchez D, Park JH, Sondermann H, Yildiz FH. 2017. The ins and outs of cyclic di-GMP signaling in Vibrio cholerae. Curr Opin Microbiol 36:20–29. https://doi.org/10.1016/j.mib.2017.01.002.
10. Srivastava D, Harris RC, Waters CM. 2011. Integration of cyclic di-GMP and quorum sensing in the control of vpsT and aphA in Vibrio cholerae. J Bacteriol 193:6331–6341. https://doi.org/10.1128/JB.05167-11.
11. Krasteva PV, Fong JCN, Shikuma NJ, Beyhan S, Navarro MVAS, Yildiz FH, Sondermann H. 2010. Vibrio cholerae VpsT regulates matrix production and motility by directly sensing cyclic di-GMP. Science 327:866–868. https://doi.org/10.1126/science.1181185.
12. Hsieh ML, Hinton DM, Waters CM. 2018. VpsR and cyclic di-GMP together drive transcription initiation to activate biofilm formation in Vibrio cholerae. Nucleic Acids Res 46:8876–8887. https://doi.org/10.1093/nar/gky606.
13. Townsley L, Yildiz FH. 2015. Temperature affects c-di-GMP signalling and biofilm formation in Vibrio cholerae. Environ Microbiol 17:4290–4305. https://doi.org/10.1111/1462-2920.12799.
14. Koestler BJ, Waters CM. 2014. Bile acids and bicarbonate inversely regulate intracellular cyclic di-GMP in Vibrio cholerae. Infect Immun 82:3002–3014. https://doi.org/10.1128/IAI.01664-14.
15. Karatan E, Duncan TR, Watnick PI. 2005. NspS, a predicted polyamine sensor, mediates activation of Vibrio cholerae biofilm formation by norspermidine. J Bacteriol 187:7434–7443. https://doi.org/10.1128/JB.187.21.7434-7443.2005.
16. Schaller RA, Ali SK, Klose KE, Kurtz DM. 2012. A bacterial hemerythrin domain regulates the activity of a Vibrio cholerae diguanylate cyclase. Biochemistry 51:8563–8570. https://doi.org/10.1021/bi3011797.
17. National Center for Biotechnology Information. 2021. Element Summary for Atomic Number 20, Calcium. PubChem. https://pubchem.ncbi.nlm.nih.gov/element/Calcium.
18. Bilecen K, Yildiz FH. 2009. Identification of a calcium-controlled negative regulatory system affecting *Vibrio cholerae* biofilm formation. Environ Microbiol 11:2015–2029. https://doi.org/10.1111/j.1462-2920.2009.01923.x.
19. Chodur DM, Coulter P, Isaacs J, Pu M, Fernandez N, Waters CM, Rowe-Magnus DA. 2018. Environmental calcium initiates a feed-forward signaling circuit that regulates biofilm formation and rugosity in Vibrio vulnificus. mBio 9:e01377-18. https://doi.org/10.1128/mBio.01377-18.
20. Tischler AH, Lie L, Thompson CM, Visick KL. 2018. Discovery of calcium as a biofilm-promoting signal for *Vibrio fischeri* reveals new phenotypes and underlying regulatory complexity. J Bacteriol 200:e00016-18. https://doi.org/10.1128/JB.00016-18.
21. Pu M, Storms E, Chodur DM, Rowe-Magnus DA. 2020. Calcium-dependent site-switching regulates expression of the atypical iam pilus locus in Vibrio vulnificus. Environ Microbiol 22:4167–4182. https://doi.org/10.1111/1462-2920.14763.
22. Guo Y, Rowe-Magnus DA. 2010. Identification of a c-di-GMP-regulated polysaccharide locus governing stress resistance and biofilm and rugose colony formation in Vibrio vulnificus. Infect Immun 78:1390–1402. https://doi.org/10.1128/IAI.01188-09.
23. Park JH, Jo Y, Jang SY, Kwon H, Irie Y, Parsek MR, Kim MH, Choi SH. 2015. The *cabABC* operon essential for biofilm and rugose colony development in *Vibrio vulnificus*. PLoS Pathog 11:e1005192. https://doi.org/10.1371/journal.ppat.1005192.
24. Chodur DM, Rowe-Magnus DA. 2018. Complex control of a genomic island governing biofilm and rugose colony development in Vibrio vulnificus. J Bacteriol 200:e00190-18. https://doi.org/10.1128/JB.00190-18.

25. O'Shea TM, Deloney-Marino CR, Shibata S, Aizawa S-I, Wolfe AJ, Visick KL. 2005. Magnesium promotes flagellation of *Vibrio fischeri*. J Bacteriol 187:2058–2065. https://doi.org/10.1128/JB.187.6.2058-2065.2005.
26. O'Shea TM, Klein AH, Geszvain K, Wolfe AJ, Visick KL. 2006. Diguanylate cyclases control magnesium-dependent motility of *Vibrio fischeri*. J Bacteriol 188:8196–8205. https://doi.org/10.1128/JB.00728-06.
27. Yip ES, Grublesky BT, Hussa EA, Visick KL. 2005. A novel, conserved cluster of genes promotes symbiotic colonization and sigma-dependent biofilm formation by Vibrio fischeri. Mol Microbiol 57:1485–1498. https://doi.org/10.1111/j.1365-2958.2005.04784.x.
28. Yip ES, Geszvain K, DeLoney-Marino CR, Visick KL. 2006. The symbiosis regulator RscS controls the *syp* gene locus, biofilm formation and symbiotic aggregation by *Vibrio fischeri*. Mol Microbiol 62:1586–1600. https://doi.org/10.1111/j.1365-2958.2006.05475.x.
29. Millikan DS, Ruby EG. 2002. Alterations in *Vibrio fischeri* motility correlate with a delay in symbiosis initiation and are associated with additional symbiotic colonization defects. Appl Environ Microbiol 68:2519–2528. https://doi.org/10.1128/AEM.68.5.2519-2528.2002.
30. Zamorano-Sánchez D, Xian W, Lee CK, Salinas M, Thongsomboon W, Cegelski L, Wong GCL, Yildiz FH. 2019. Functional specialization in *Vibrio cholerae* diguanylate cyclases: distinct modes of motility suppression and c-di-GMP production. mBio 10:e00670-19. https://doi.org/10.1128/mBio.00670-19.
31. Ruby EG, Urbanowski M, Campbell J, Dunn A, Faini M, Gunsalus R, Lostroh P, Lupp C, McCann J, Millikan D, Schaefer A, Stabb E, Stevens A, Visick K, Whistler C, Greenberg EP. 2005. Complete genome sequence of *Vibrio fischeri*: a symbiotic bacterium with pathogenic congeners. Proc Natl Acad Sci U S A 102:3004–3009. https://doi.org/10.1073/pnas.0409900102.
32. Wolfe AJ, Visick KL. 2010. Roles of diguanylate cyclases and phosphodiesterases in motility and biofilm formation in Vibrio fischeri, p 186–200. *In* Wolfe AJ, Visick KL (ed), The second messenger cyclic-di-GMP. ASM Press, Washington, DC.
33. Mandel MJ, Stabb EV, Ruby EG. 2008. Comparative genomics-based investigation of resequencing targets in *Vibrio fischeri*: focus on point miscalls and artefactual expansions. BMC Genomics 9:138. https://doi.org/10.1186/1471-2164-9-138.
34. Shimomura O, Johnson FH, Saiga Y. 1962. Extraction, purification and properties of aequorin, a bioluminescent protein from the luminous hydromedusan, Aequorea. J Cell Comp Physiol 59:223–239. https://doi.org/10.1002/jcp.1030590302.
35. Shimomura O, Johnson FH. 1969. Properties of the bioluminescent protein aequorin. Biochemistry 8:3991–3997. https://doi.org/10.1021/bi00838a015.
36. Rasband WS. 1997. ImageJ. US National Institutes of Health, Bethesda, MD.
37. Zorraquino V, García B, Latasa C, Echeverz M, Toledo-Arana A, Valle J, Lasa I, Solano C. 2013. Coordinated cyclic-di-GMP repression of Salmonella motility through YcgR and cellulose. J Bacteriol 195:417–428. https://doi.org/10.1128/JB.01789-12.
38. Darnell CL, Hussa EA, Visick KL. 2008. The putative hybrid sensor kinase SypF coordinates biofilm formation in *Vibrio fischeri* by acting upstream of two response regulators, SypG and VpsR. J Bacteriol 190:4941–4950. https://doi.org/10.1128/JB.00197-08.
39. Dutta R, Inouye M. 2000. GHKL, an emergent ATPase/kinase superfamily. Trends Biochem Sci 25:24–28. https://doi.org/10.1016/S0968-0004(99)01503-0.
40. Parkinson JS, Kofoid EC. 1992. Communication modules in bacterial signaling proteins. Annu Rev Genet 26:71–112. https://doi.org/10.1146/annurev.ge.26.120192.000443.
41. Altschul SF, Gish W, Miller W, Myers EW, Lipman DJ. 1990. Basic local alignment search tool. J Mol Biol 215:403–410. https://doi.org/10.1016/S0022-2836(05)80360-2.
42. Pidcock E, Moore GR. 2001. Structural characteristics of protein binding sites for calcium and lanthanide ions. J Biol Inorg Chem 6:479–489. https://doi.org/10.1007/s007750100214.
43. Shikuma NJ, Fong JC, Yildiz FH. 2012. Cellular levels and binding of c-di-GMP control subcellular localization and activity of the Vibrio cholerae transcriptional regulator VpsT. PLoS Pathog 8:e1002719. https://doi.org/10.1371/journal.ppat.1002719.
44. Ross P, Aloni Y, Weinhouse C, Michaeli D, Weinberger-Ohana P, Meyer R, Benziman M. 1985. An unusual guanyl oligonucleotide regulates cellulose synthesis in Acetobacter xylinum. FEBS Lett 186:191–196. https://doi.org/10.1016/0014-5793(85)80706-7.
45. Aloni Y, Cohen R, Benziman M, Delmer D. 1983. Solubilization of the UDP-glucose:1,4-beta-D-glucan 4-beta-D-glucosyltransferase (cellulose synthase) from Acetobacter xylinum. A comparison of regulatory properties with those of the membrane-bound form of the enzyme. J Biol Chem 258:4419–4423. https://doi.org/10.1016/S0021-9258(18)32639-5.
46. Advani MJ, Rajagopalan M, Reddy PH. 2014. Calmodulin-like protein from M. tuberculosis H37Rv is required during infection. Sci Rep 4:6861. https://doi.org/10.1038/srep06861.
47. Koul S, Somayajulu A, Advani MJ, Reddy H. 2009. A novel calcium binding protein in Mycobacterium tuberculosis—potential target for trifluoperazine. Indian J Exp Biol 47:480–488.
48. King MM, Kayastha BB, Franklin MJ, Patrauchan MA. 2020. Calcium regulation of bacterial virulence. Adv Exp Med Biol 1131:827–855. https://doi.org/10.1007/978-3-030-12457-1_33.
49. Boyd CD, Chatterjee D, Sondermann H, O'Toole GA. 2012. LapG, required for modulating biofilm formation by *Pseudomonas fluorescens* Pf0-1, is a calcium-dependent protease. J Bacteriol 194:4406–4414. https://doi.org/10.1128/JB.00642-12.
50. Chatterjee D, Boyd CD, O'Toole GA, Sondermann H. 2012. Structural characterization of a conserved, calcium-dependent periplasmic protease from Legionella pneumophila. J Bacteriol 194:4415–4425. https://doi.org/10.1128/JB.00640-12.
51. Salah Ud-Din AIM, Roujeinikova A. 2017. Methyl-accepting chemotaxis proteins: a core sensing element in prokaryotes and archaea. Cell Mol Life Sci 74:3293–3303. https://doi.org/10.1007/s00018-017-2514-0.
52. Römling U, Galperin MY. 2015. Bacterial cellulose biosynthesis: diversity of operons, subunits, products, and functions. Trends Microbiol 23:545–557. https://doi.org/10.1016/j.tim.2015.05.005.
53. Zogaj X, Nimtz M, Rohde M, Bokranz W, Romling U. 2001. The multicellular morphotypes of *Salmonella typhimurium* and *Escherichia coli* produce cellulose as the second component of the extracellular matrix. Mol Microbiol 39:1452–1463. https://doi.org/10.1046/j.1365-2958.2001.02337.x.
54. Thongsomboon W, Serra DO, Possling A, Hadjineophytou C, Hengge R, Cegelski L. 2018. Phosphoethanolamine cellulose: a naturally produced chemically modified cellulose. Science 359:334–338. https://doi.org/10.1126/science.aao4096.
55. Chan C, Paul R, Samoray D, Amiot NC, Giese B, Jenal U, Schirmer T. 2004. Structural basis of activity and allosteric control of diguanylate cyclase. Proc Natl Acad Sci U S A 101:17084–17089. https://doi.org/10.1073/pnas.0406134101.
56. Bassis CM, Visick KL. 2010. The cyclic-di-GMP phosphodiesterase BinA negatively regulates cellulose-containing biofilms in *Vibrio fischeri*. J Bacteriol 192:1269–1278. https://doi.org/10.1128/JB.01048-09.
57. Casper-Lindley C, Yildiz FH. 2004. VpsT is a transcriptional regulator required for expression of *vps* biosynthesis genes and the development of rugose colonial morphology in *Vibrio cholerae* O1 El Tor. J Bacteriol 186:1574–1578. https://doi.org/10.1128/JB.186.5.1574-1578.2004.
58. Boettcher KJ, Ruby EG. 1990. Depressed light emission by symbiotic *Vibrio fischeri* of the sepiolid squid *Euprymna scolopes*. J Bacteriol 172:3701–3706. https://doi.org/10.1128/jb.172.7.3701-3706.1990.
59. Le Roux F, Binesse J, Saulnier D, Mazel D. 2007. Construction of a *Vibrio splendidus* mutant lacking the metalloprotease gene *vsm* by use of a novel counterselectable suicide vector. Appl Environ Microbiol 73:777–784. https://doi.org/10.1128/AEM.02147-06.
60. Graf J, Dunlap PV, Ruby EG. 1994. Effect of transposon-induced motility mutations on colonization of the host light organ by *Vibrio fischeri*. J Bacteriol 176:6986–6991. https://doi.org/10.1128/jb.176.22.6986-6991.1994.
61. Stabb EV, Reich KA, Ruby EG. 2001. *Vibrio fischeri* genes *hvnA* and *hvnB* encode secreted NAD(+)-glycohydrolases. J Bacteriol 183:309–317. https://doi.org/10.1128/JB.183.1.309-317.2001.
62. Davis RW, Botstein D, Roth JR. 1980. A manual for genetic engineering, advanced bacterial genetics. Cold Spring Harbor Laboratory Press, Cold Spring Harbor, NY.
63. Pollack-Berti A, Wollenberg MS, Ruby EG. 2010. Natural transformation of *Vibrio fischeri* requires *tfoX* and *tfoY*. Environ Microbiol 12:2302–2311.
64. Brooks JF, Gyllborg MC, Cronin DC, Quillin SJ, Mallama CA, Foxall R, Whistler C, Goodman AL, Mandel MJ, II. 2014. Global discovery of colonization determinants in the squid symbiont *Vibrio fischeri*. Proc Natl Acad Sci U S A 111:17284–17289. https://doi.org/10.1073/pnas.1415957111.
65. Christensen DG, Tepavcevic J, Visick KL. 2020. Genetic manipulation of *Vibrio fischeri*. Curr Protoc Microbiol 59:e115. https://doi.org/10.1002/cpmc.115.
66. Cohen JJ, Eichinger SJ, Witte DA, Cook CJ, Fidopiastis PM, Tepavčević J, Visick KL. 2021. Control of competence in *Vibrio fischeri*. Appl Environ Microbiol 87:e01962-20. https://doi.org/10.1128/AEM.01962-20.
67. Horton RM, Hunt HD, Ho SN, Pullen JK, Pease LR. 1989. Engineering hybrid genes without the use of restriction enzymes: gene splicing by overlap extension. Gene 77:61–68. https://doi.org/10.1016/0378-1119(89)90359-4.

68. Visick KL, Hodge-Hanson KM, Tischler AH, Bennett AK, Mastrodomenico V. 2018. Tools for rapid genetic engineering of Vibrio fischeri. Appl Environ Microbiol 84:e00850-18. https://doi.org/10.1128/AEM.00850-18.
69. McCann J, Stabb EV, Millikan DS, Ruby EG. 2003. Population dynamics of *Vibrio fischeri* during infection of *Euprymna scolopes*. Appl Environ Microbiol 69:5928–5934. https://doi.org/10.1128/AEM.69.10.5928-5934.2003.
70. Stabb EV, Ruby EG. 2002. RP4-based plasmids for conjugation between *Escherichia coli* and members of the Vibrionaceae. Methods Enzymol 358:413–426. https://doi.org/10.1016/S0076-6879(02)58106-4.
71. Bao Y, Lies DP, Fu H, Roberts GP. 1991. An improved Tn7-based system for the single-copy insertion of cloned genes into chromosomes of gram-negative bacteria. Gene 109:167–168. https://doi.org/10.1016/0378-1119(91)90604-A.
72. Cherepanov PP, Wackernagel W. 1995. Gene disruption in *Escherichia coli*: TcR and KmR cassettes with the option of Flp-catalyzed excision of the antibiotic-resistance determinant. Gene 158:9–14. https://doi.org/10.1016/0378-1119(95)00193-A.
73. Dunn AK, Millikan DS, Adin DM, Bose JL, Stabb EV. 2006. New rfp- and pES213-derived tools for analyzing symbiotic Vibrio fischeri reveal patterns of infection and lux expression in situ. Appl Environ Microbiol 72:802–810. https://doi.org/10.1128/AEM.72.1.802-810.2006.
74. Miller JH. 1972. Experiments in molecular genetics. Cold Spring Harbor Laboratory, Cold Spring Harbor, NY.
75. Kumari S, Beatty CM, Browning DF, Busby SJ, Simel EJ, Hovel-Miner G, Wolfe AJ. 2000. Regulation of acetyl coenzyme A synthetase in Escherichia coli. J Bacteriol 182:4173–4179. https://doi.org/10.1128/JB.182.15.4173-4179.2000.
76. Bose JL, Rosenberg CS, Stabb EV. 2008. Effects of *luxCDABEG* induction in *Vibrio fischeri*: enhancement of symbiotic colonization and conditional attenuation of growth in culture. Arch Microbiol 190:169–183. https://doi.org/10.1007/s00203-008-0387-1.
77. Norsworthy AN, Visick KL. 2015. Signaling between two interacting sensor kinases promotes biofilms and colonization by a bacterial symbiont. Mol Microbiol 96:233–248. https://doi.org/10.1111/mmi.12932.
78. Visick KL, Skoufos LM. 2001. Two-component sensor required for normal symbiotic colonization of *Euprymna scolopes* by *Vibrio fischeri*. J Bacteriol 183:835–842. https://doi.org/10.1128/JB.183.3.835-842.2001.